OROGRAPHY AND THE DEVELOPMENT OF THE ECMWF FORECAST MODEL

A.J. Simmons
European Centre for Medium Range Weather Forecasts
Reading, U.K.

1. INTRODUCTION

Questions concerning the prescription of the model orography and related aspects of the numerical formulation and parameterization of sub-gridscale effects have been to the fore in the development of the ECMWF model in the seven years since the start of operational forecasting at the Centre. Many of the topics considered have already been discussed to a greater or lesser extent in other contributions to these proceedings; consequently in this paper no attempt will be made to give an introductory review of the subjects to be presented or to compare and contrast the approaches and experiences of ECMWF with those of other forecasting centres. Rather, the aim is simply to provide an account of how the presence of mountains has influenced, and continues to influence, the development of the ECMWF forecast model.

The following section describes the five different specifications of orography that have been used in operational forecasting. It is followed by discussion of a number of aspects of the numerical formulation which have received attention because of problems associated with orography. The topics presented are the choice of vertical coordinate and calculation of pressure gradients, the advection of moisture, horizontal diffusion and precipitation, and the choice of prognostic variables in spectral models. The papers by Jarraud et al. and by Miller and Palmer in this volume provide detailed information on the use of envelope orography and the parameterization of gravity-wave drag in the current ECMWF model; additional comment is given here in Section 4. This is followed by some discussion of the representation of orography in higher horizontal resolution models.

2. MODEL OROGRAPHIES

The orography used for the initial phase of operational forecasting, which began on 1 August 1979, was interpolated to the grid of the N48 (1.875°) resolution finite-difference model (Burridge and Haseler, 1977) from the coarser N24 (3.75°) grid of a dataset made available to ECMWF by the Geophysical Fluid Dynamics Laboratory, Princeton, USA. This orography in turn

was based on a dataset produced by Berkofsky and Bertoni (1955) who tabulated mean heights by eye over one-degree grid-squares, and subsequently averaged the results to obtain a 5° resolution field. The resulting model orography thus represented the larger-scale features of the actual orography, but its resolution was insufficient to describe adequately a number of mountain ranges known to have an important influence on synoptic-scale motion, for example through triggering lee cyclogenesis. The upper left panel of Figure 1 compares a north-south section of this model orography with high-resolution data near 10°E, and illustrates how the Alpine mountain barrier was almost completely absent in the first operational orography. Already in 1979, the production of a more realistic orography and assessment of its impact had begun.

Operational change resulted in April 1981. As documented by Tibaldi and Geleyn (1981), the new orography was based on a dataset of orographic and other surface characteristics produced by the US Navy and made available to ECMWF through the National Center for Atmospheric Research, U.S.A. The N48 resolution orography was computed by averaging for each model grid-square the mean surface elevations of 10' resolution grid squares. The resulting heights were smoothed slightly using a bi-dimensional Gaussian filter with a radius of 100 km. The Alpine section for this N48 orography is compared with the 10' mean section in the upper-right plot of Figure 1; the increase in resolution over the original operational orography is evident, although the ridge height remains seriously underestimated. Experimental testing of the orographic change led to expectation of a general beneficial operational impact, at least beyond the four-day range, and improved lee cyclogenesis was anticipated. The volume of experimentation that could be carried out in support of the change was, however, insufficient to give a reliable quantitative indication of the degree of improvement.

A continuing systematic tendency for the operational forecasts to fail to maintain the amplitude of the upper-level quasi-stationary wave pattern caused further investigation of the representation of orography in the model. The work of Wallace et al. (1983) on the diagnosis of forecast error which led to adoption of a higher "envelope" orography has already been introduced by Jarraud et al. in these proceedings. At the same time, a spectral model was being developed for operational forecasting (Simmons and Jarraud, 1984), and

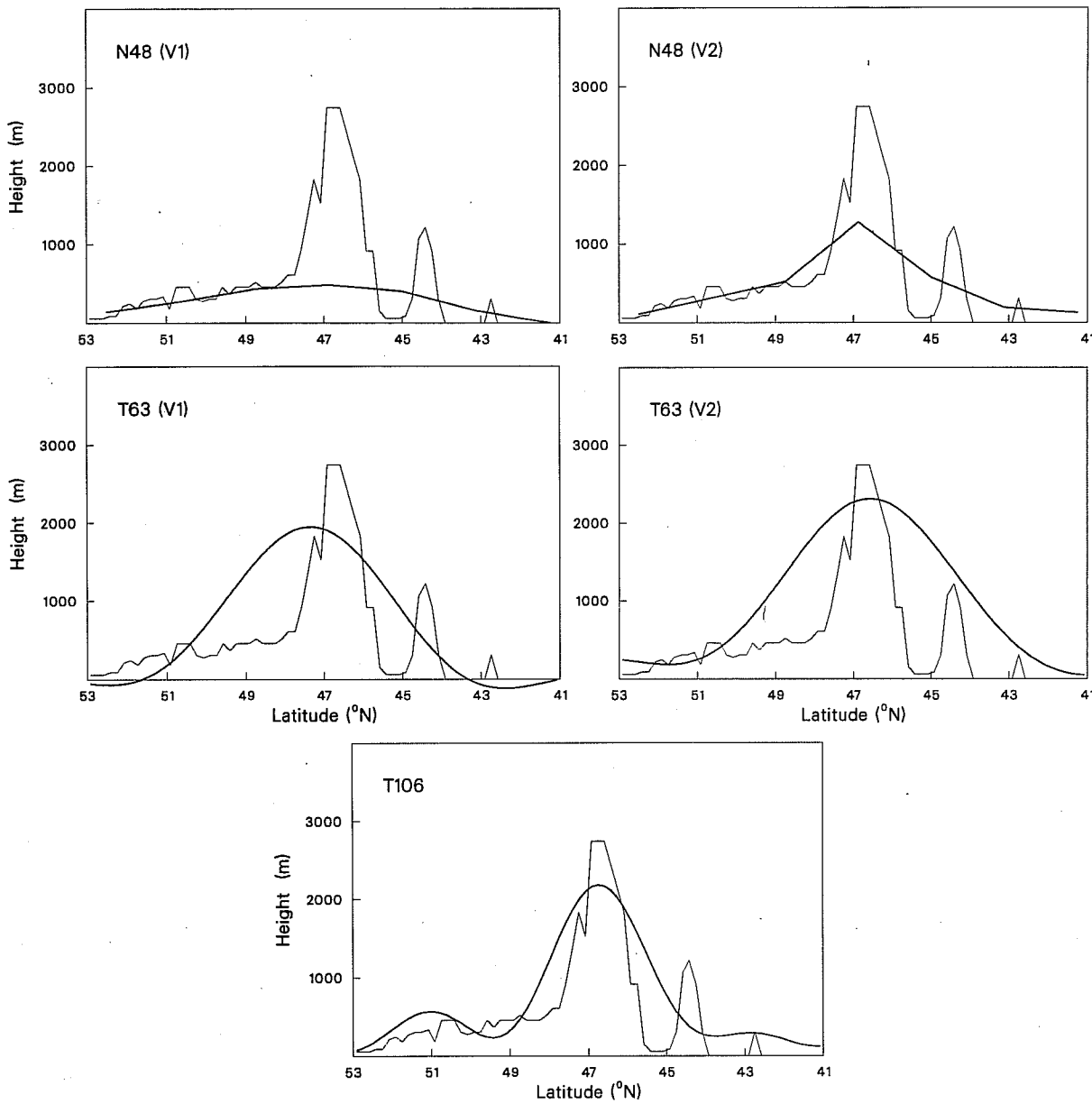

Fig. 1 Orographic cross-sections from 53°N to 41°N at 10°5'E. The fine lines in each plot depict mean heights of 10' x 10' grid squares from a dataset made available by the US Navy. The heavier lines denote the model orographies that have been used operationally at ECMWF. Details are given in the text.

with its implementation in April 1983 the operational orography became a spectrally-fitted envelope orography. This was formed by adding to the grid-square mean, computed on the model's 192 x 96 point Gaussian grid, $\sqrt{2}$ times the standard deviation of the sub-gridscale orographic distribution, as calculated from the high resolution US Navy data. The resulting grid-point field was then represented by a spectral expansion truncated triangularly at total wavenumber 63, the resolution of the first operational version of the spectral model.

Earlier tests in data assimilation had shown that use of the higher envelope orography generally resulted in an increase in the number of observations from coastal stations that were discarded by the analysis because of significant discrepancies between the height of the station and that of the model orography. The basic spectrally-fitted envelope orography was thus modified in an iterative procedure which restored sea points (points with more than 50% of the grid-square sea in reality) to zero height between successive spectral fits of the orography as evaluated on the model's Gaussian grid. The new orography gave fewer coastal data rejections. However, this was achieved at the expense of unrealistically lowering heights immediately inland. Early operational experience suggested that this was detrimental to the systematic errors of the height and precipitation fields. Indeed, subsequent tests by Jarraud (personal communication) indicated that the lowering of heights inland more than countered any advantages of increased data acceptance, and in February 1984 a new orography was introduced operationally. This comprised a single (non-iterated) spectral fit to the $\sqrt{2}$ standard-deviation envelope orography computed on the Gaussian grid, but with the envelope increment added to the mean only at grid-squares designated as land in the model.

Alpine sections for the two operational T63 orographies are presented in the middle plots of Figure 1. The increased elevation due to the envelope is clearly seen, but the limited horizontal resolution is such that the improved ridge height is achieved at the expense of an unrealistic lateral spreading of the mountain range. The original, iterated orography (middle left) displays a reduction in height south of about 48°N because the repeated zeroing of heights over the Mediterranean during the iteration process appears to cause a northward shift in the position of the Alps.

The final section shown in Figure 1 illustrates the orography used since May 1985 in the operational, T106 version of the spectral model. It is an envelope orography based on adding one rather than $\sqrt{2}$ standard deviations of the sub-gridscale mountain distribution. For the section illustrated, the maximum height of this higher resolution orography is similar to that of the $\sqrt{2}$ envelope at T63 resolution, but the unrealistic spreading is much reduced. Evidence supporting this choice of orography is presented by Jarraud et al. in this volume. The T106 envelope was constructed in the same way as the second of the T63 orographies, apart from the inclusion of a weak Gaussian filtering, (with 50 km radius) carried out in grid-point space prior to the spectral fit. Tests showed this to have a negligible impact on the synoptic-scale forecasts but it produced a quite significant reduction in the inevitable ripples in the spectrally-fitted orography over sea, and thus noticeably reduced related biases in precipitation which could reach several millimetres per day.

3. ASPECTS OF THE NUMERICAL FORMULATION

3.1 Introduction

The presence of orography in a forecast model strongly influences the choice of vertical coordinate and related aspects of the numerical formulation. It has become increasingly common to use terrain-following coordinate surfaces for which the lower boundary condition assumes a relatively simple form at the expense of a number of problems associated with steeply-sloping coordinate surfaces. Some of the problems that have been investigated for the ECMWF model are discussed in the following sections.

3.2 The vertical coordinate and pressure-gradient calculation

The classical sigma coordinate, pressure divided by its surface value, proposed by Phillips (1957) was adopted in the first operational ECMWF model. A 15-layer resolution was used; the distribution of "full" levels at which the prognostic upper-air variables were located is shown schematically in the upper plot in Figure 2. Work elsewhere had, however, already identified a number of deficiencies of this coordinate, and an investigation was thus begun into the use of "hybrid" coordinates which changes from being terrain-following at low levels to a pressure coordinate at upper levels. Results reported by Simmons and Burridge (1981) and Simmons and Strüfing (1981) showed how some of the problems with sigma coordinates could be removed

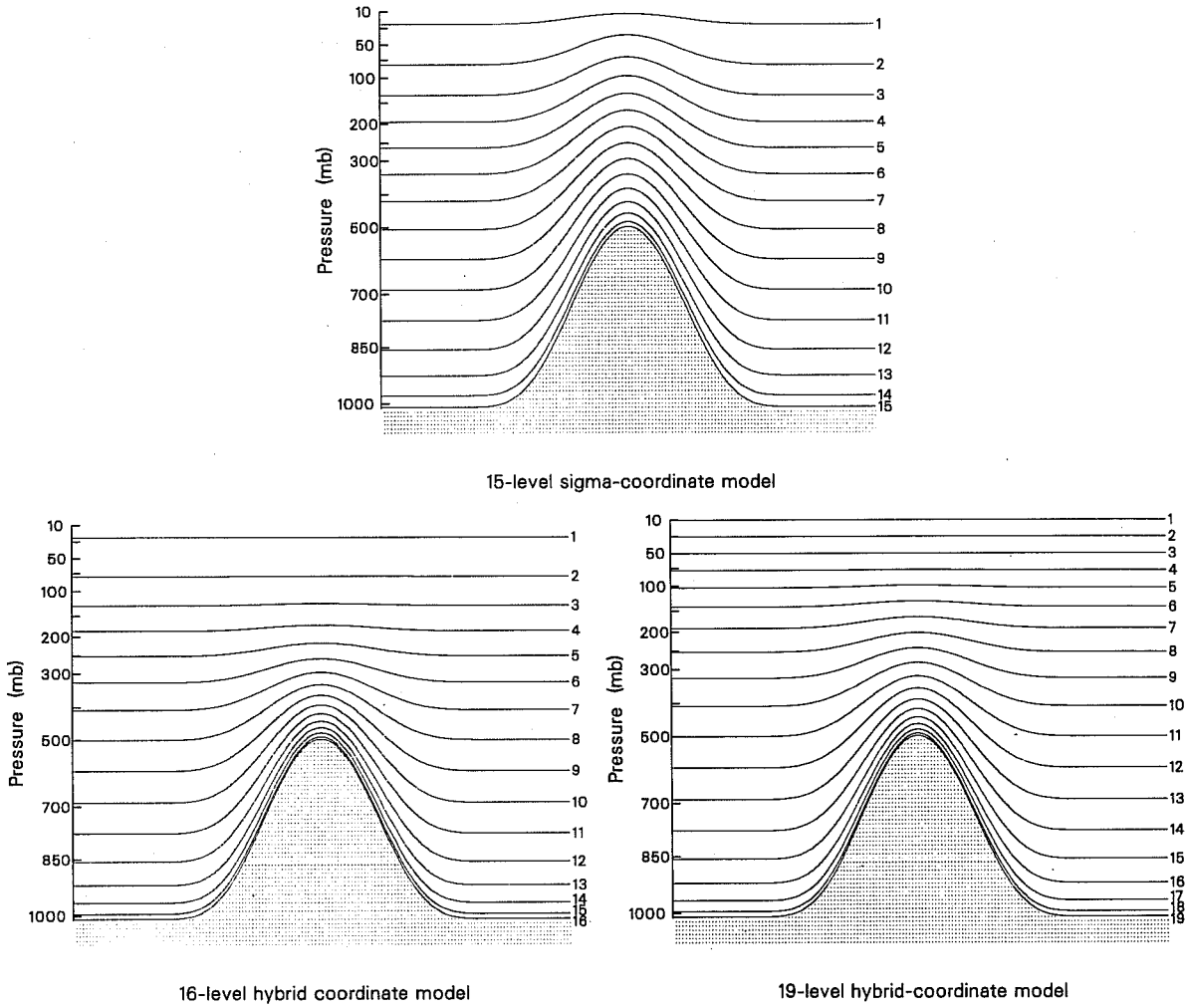

Fig. 2 Vertical coordinates and resolutions that have been used operationally.

or alleviated with little penalty by use of a coordinate which changed gradually from sigma to pressure from the boundary layer to the lower stratosphere. Such a coordinate was introduced operationally at the time of the change to the spectral model, and is illustrated in the lower left plot of Figure 2. Vertical resolution over the sea was essentially unchanged, apart from addition of an extra level within the boundary layer for reasons of consistency of formulation (Simmons, 1983).

One disadvantage of the sigma coordinate is that it necessitates, in general, vertical interpolation of model data to pressure levels to provide a first guess for the data assimilation, and for purposes of presentation, diagnosis and archiving of results. The vertical resolution first used with the hybrid coordinate was such as to remove some of the biases over orography in stratospheric pressure-level fields caused by differences in the extent of vertical interpolation from sigma-level data. However, vertical interpolation from model levels to the standard pressure levels continued to give rise to problems, particularly in stratospheric data assimilation. Fuller benefits of the hybrid coordinate were attained in May 1986 with the operational introduction of the 19-level vertical resolution shown lower right in Figure 2. Model levels are now located precisely at 10 and 30 hPa, and are very close to standard pressure levels lower in the stratosphere. Distinct improvements in data assimilation, and subsequent forecasts, have been noted by Wergen and Simmons (1986).

Perhaps the problem with terrain-following coordinates that has been most discussed in the literature is that of the calculation of the pressure gradient:

$$\nabla_\eta \phi + RT \nabla_\eta \ell np$$

with ϕ the geopotential, R the gas constant, T the temperature, p the pressure, and ∇_η the operator representing the gradient with respect to longitude and latitude computed along the (sigma or hybrid) coordinate surfaces of the model. Where these surfaces rise up over steeply sloping orography, the above two terms exhibit a strong cancellation which cannot in general be perfectly achieved numerically. The problem is reduced at upper levels by use of the hybrid coordinate, although even at pressure levels, where only the $\nabla\phi$ term remains, a spurious pressure gradient can result from inevitable differences in the vertical integration to compute ϕ at points with

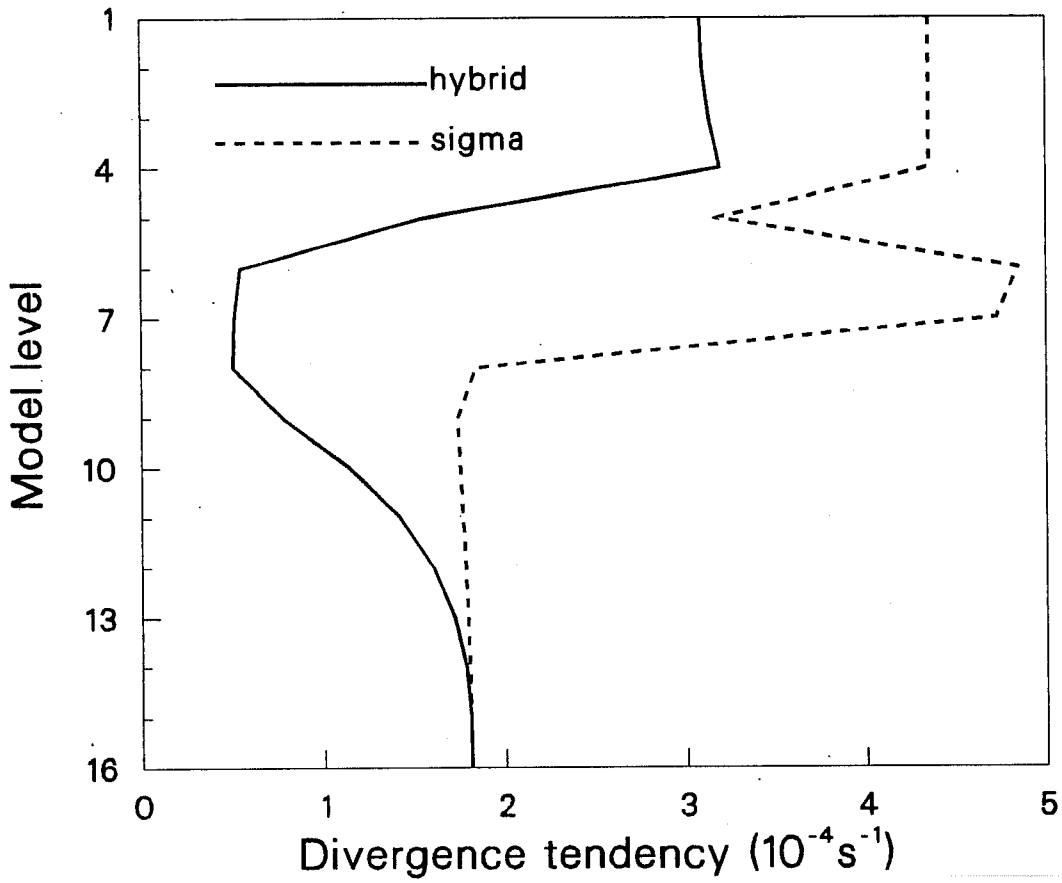

Fig. 3 The maximum spurious initial divergence tendency computed over all model grid-points for the 16-level resolution shown in Fig. 2, for a dry atmosphere at rest with temperature prescribed analytically as a function of height, z, by
$T = 288 - .0065z$ for $z < 11 \times 10^3$ m
$= 216.5$ otherwise.
The solid line denotes the result for the operational hybrid coordinate and the dashed line the result for the sigma coordinate which coincides with the hybrid coordinate at sea level. Other details are given in the text.

different surface elevations. An illustration is given in Figure 3; this presents the maximum erroneous initial divergence tendency at each level of a global T63 model with the second operational spectral orography for a dry atmosphere at rest in which the analytically-prescribed temperature varies only with pressure as in the ICAO standard atmosphere. The lower error with the hybrid coordinate is clear, even after allowing for a misleading impression for levels 6 and 7 which, for the sigma but not the hybrid coordinate, intersect the tropopause where error increases sharply.

In addition to changes necessitated by the introduction of the hybrid vertical coordinate, a further minor change to the vertical finite difference scheme of the model was made in April 1983. This ensured that the angular momentum of the model atmosphere changed by precisely the amount given by the model mountain torque, apart from errors due to the horizontal and temporal discretization. Details are given by Simmons and Strüfing (1981) who show that this scheme also yields a more accurate local pressure-gradient calculation than two hybrid-coordinate discretizations of algebraically simpler form.

3.3 Advection of moisture

The pressure gradient is not the only term in the governing equations which can suffer from inaccurate calculation where coordinate surfaces slope steeply. In particular, consider purely horizontal advection of any variable, X say, which varies in the vertical. If coordinate surfaces slope, this advection will be represented by two terms in the model:

$$\underline{u}.\nabla_\eta X + \dot{\eta}\,\frac{\partial X}{\partial \eta}$$

Here the first term appears as (and is usually referred to as) a "horizontal" advection, with $\underline{u}$ the horizontal velocity, but the gradient is taken along the coordinate surface. The second term appears as a "vertical advection", η being the vertical coordinate and $\dot{\eta}$ its material rate of change, which is proportional to the surface-pressure gradient in the idealized case of spatially uniform flow. If X varies only in the vertical, the two terms should cancel. Numerical problems in achieving this are likely to be most severe for quantities which vary rapidly in the vertical, specific humidity (the prognostic moisture variable in the ECMWF model) being the prime example.

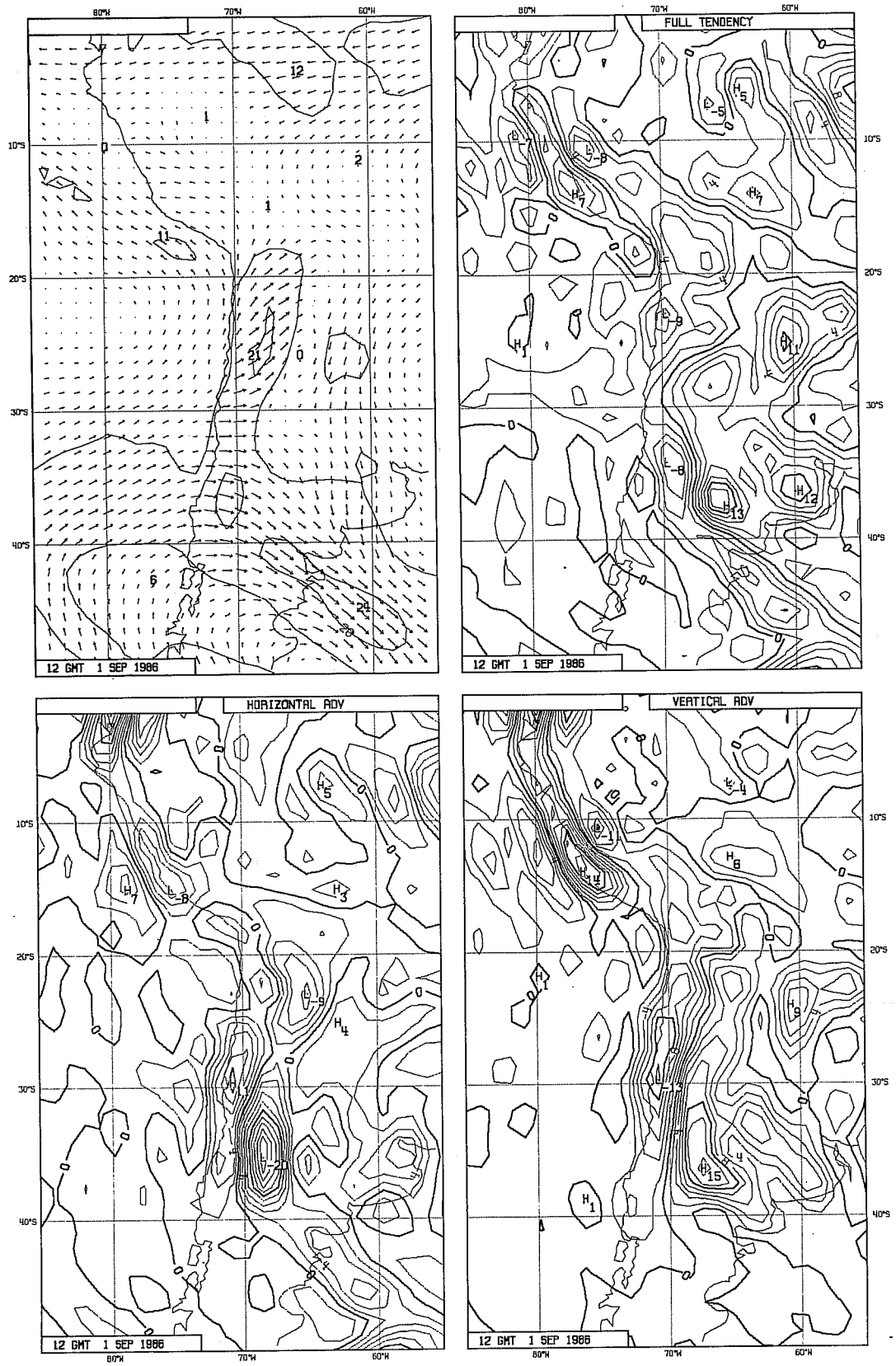

Fig. 4 Initial fields for 12Z, 1 September, 1986 for model level 13 in the vicinity of the Andes. The horizontal wind (in ms^{-1}) and dynamical tendency of specific humidity (in g Kg^{-1} day^{-1}) are shown upper left and right, respectively. Contributions to the tendency from "horizontal" and "vertical" advection are shown lower left and right.

Soon after operational implementation of the spectral model, a detailed study of some balances near the Andes and the coast of Greenland was necessitated by an intermittent severe cooling of the land surface. As a by-product, it was realised that on occasions the dynamical calculation of the model was producing strong tendencies towards unphysical negative specific humidities in these (and perhaps other) steeply mountainous regions. The general priorities of model development have been such that this unrealistic behaviour has not yet been investigated further. However, to illustrate the tendency for cancellation between the two advection terms, Figure. 4 shows a number of fields at model level 13 (about 700 hPa over the oceans) computed from the uninitialised operational analysis for 12Z, 1 September 1986, over a domain including much of the Andes. The upper panels show the horizontal wind and net dynamical tendency of specific humidity. The "horizontal" and "vertical" advection terms which comprise the net tendency are shown in the lower panels. Near the Andes, these latter two fields are similar in pattern and opposite in sign, and it is difficult to know what confidence can be placed in the residual net tendency. Full study of this problem, in particular of any systematic errors in moisture advection, would appear to be worthwhile.

3.4 Horizontal diffusion and precipitation

A problem with terrain-following coordinates occurs also with respect to the "horizontal" diffusion that is generally included in numerical prediction models. It is most convenient to perform this diffusion along the model coordinate surfaces. Where these slope steeply, and the diffusion is applied to temperature and specific humidity as prognostic variables, there is a tendency to warm and moisten the atmosphere above the higher ground, and this can act to trigger convection. No particular problems of this nature were experienced with the Centre's grid-point model when the original, highly smoothed orography was used, but excessive convective precipitation over mountain areas (and in particular over the Alps in summer) was found when the grid-square mean orography was introduced. Using such an orography in the hybrid-coordinate spectral model gave much less of a problem, but rainfall biases were again evident when the envelope orography was used with this model.

Two solutions to the problem are either to apply the diffusion to variables which have a much more uniform distribution in the vertical, or to apply the

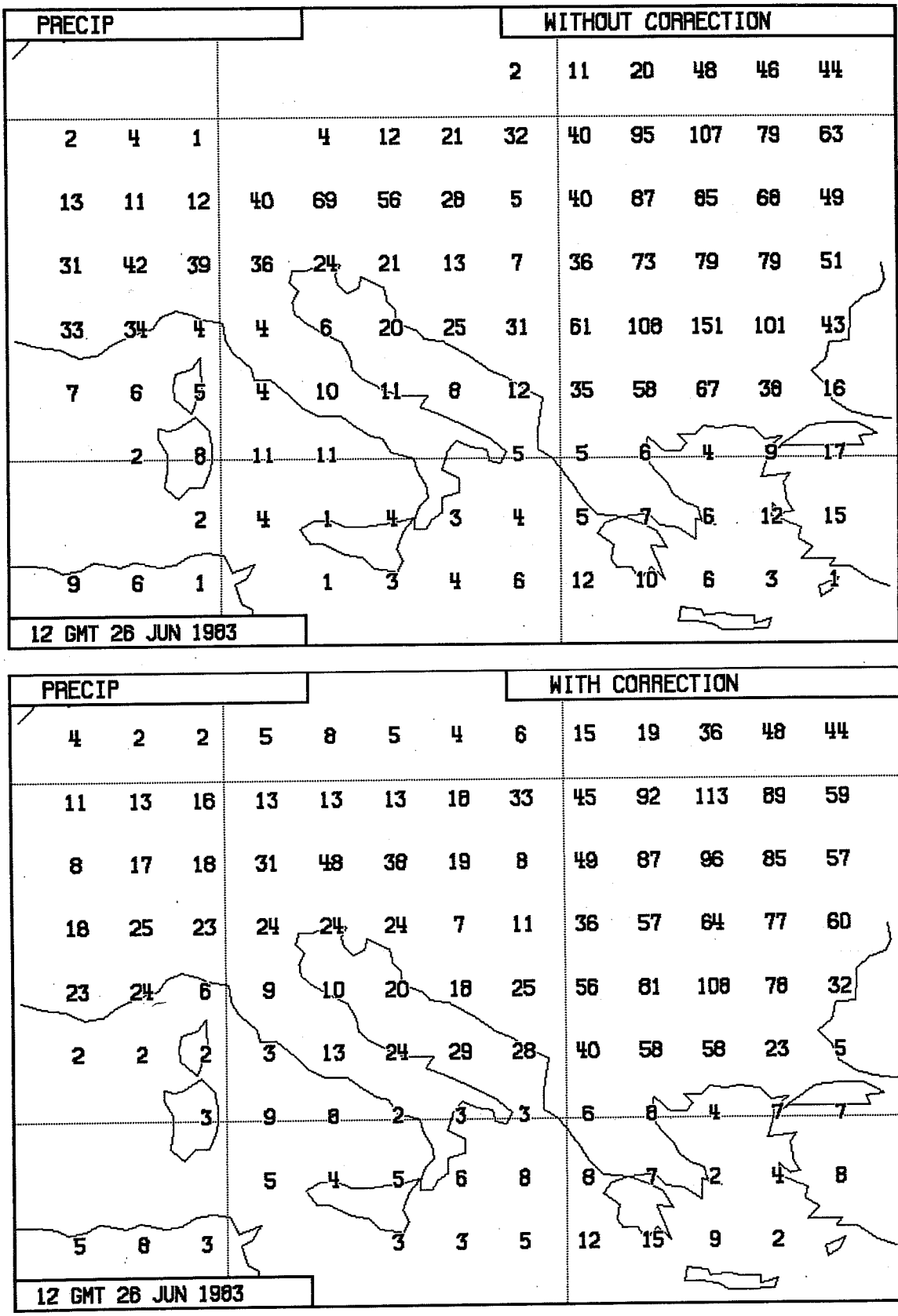

Fig. 5 Precipitation accumulated over Southern Europe in two 10-day T63 forecasts, plotted in mm for each model grid square. The upper plot is for full temperature diffusion, and the lower plot shows the results obtained with the correction to reduce excess orographic precipitation.

diffusion in a more truly horizontal plane. Experience shows that it is the treatment of the temperature field which is the most crucial. The solution adopted for the ECMWF spectral model, which uses linear, 4th-order diffusion, is to diffuse not the full temperature, T, but rather

$$T - \left(p_s \frac{\partial p}{\partial p_s} \frac{\partial T}{\partial p}\right)_{ref} \ell n p_s$$

where p_s is the surface pressure and $(\quad)_{ref}$ denotes reference values, derived from the ICAO standard atmosphere, which vary only with the model level. This approximates diffusion of temperature on pressure surfaces (particularly for small deviations from the reference temperature and small surface pressure variations) and, because it involves a linear combination of variables, it is simple and cheap to implement in spectral space.

Figure 5 shows precipitation accumulated over sample 10-day T63 forecasts carried out using diffusion of the full temperature (upper) and the modified diffusion specified above (lower). The correction term which serves to approximate diffusion on pressure surfaces evidently results in a reduction in precipitation maxima over the Alps and southeastern Europe. Precipitation is increased slightly over neighbouring areas. These and other cases reveal little sensitivity of the synoptic-scale motion to the form of diffusion.

Although the operational implementation of the modified diffusion resulted in a major reduction in the precipitation bias in mountainous regions, some bias still remains. Routine comparison of day-3 operational forecasts with data from synoptic stations currently reveals a distinct tendency for overprediction of precipitation in the Alpine region. The problems discussed in this and the preceding section may still be playing a rôle, but there are other factors discussed elsewhere in this volume which can also contribute to bias in the verification of precipitation near mountains.

3.5 The spectral representation of the surface-pressure variable

The Centre's spectral model, in common with most other such models, is based on use of a spectral representation for the logarithm of surface pressure rather than surface pressure itself. This has some computational advantage for a model with sigma coordinates, but the advantage disappears for the hybrid coordinate currently used. Indeed, use of p_s rather than $\ell n p_s$ as the prognostic spectral variable has the advantage of a somewhat more stable semi-implicit scheme for hybrid coordinates (Simmons and Strüfing, 1981), and

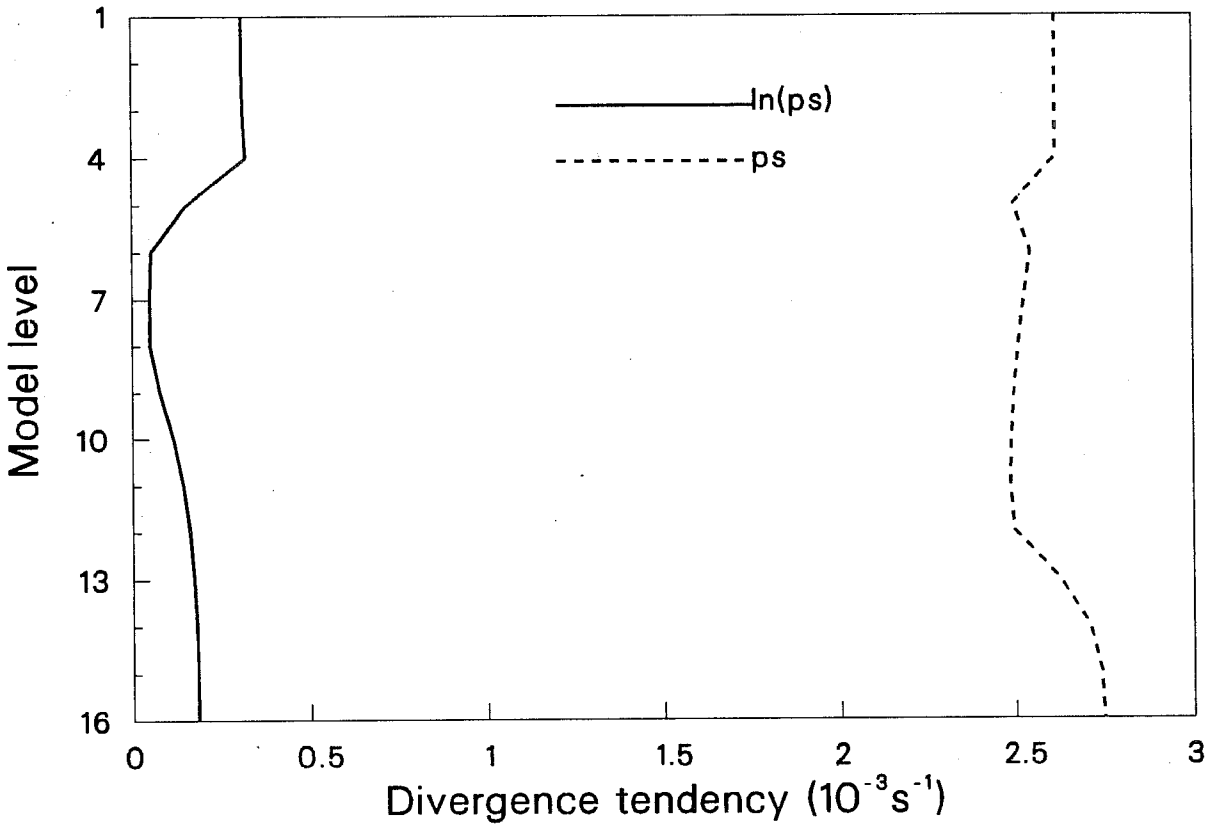

Fig. 6 Spurious initial divergence tendencies as in Fig. 3, but for the hybrid coordinate with ℓnp_s (solid) and p_s (dashed) as spectrally-represented variables.

leads directly to a mass-conserving scheme (Gordon, 1981). Mass change during a typical 10 day operational forecast is quite insignificant with the ℓnp_s formulation, but can be serious when lower resolution spectral models are integrated well beyond a year in climate simulations (Cubasch, personal communication, Laprise, 1981).

Although testing of p_s as a prognostic variable has yet to result in operational implementation of such a scheme, it is instructive to examine some of the results of these tests as they provide an example of insensitivity to a locally inaccurate representation of the pressure gradient.

Introducing the change to p_s without making any adjustments to the basic numerical formulation gives rise to a marked increase in error in the pressure-gradient calculation. Figure 6 shows the result of the same calculation as presented in Figure 3, but now for the hybrid coordinate alone, and for ℓnp_s and p_s as prognostic variables. The erroneous divergence tendency can be seen to be an order of magnitude larger when p_s is the spectrally-represented variable. This can be readily appreciated by considering the second of the two terms which comprise the net gradient:

$$RT\ \nabla_\eta \ell np$$

At low levels, where the vertical coordinate is effectively sigma, this is calculated in the ℓnp_s scheme as

$$RT\ \nabla \ell np_s$$

and (apart from virtual temperature effects) this term is a simple product of two spectrally-represented terms. With p_s as the variable, the term is computed as

$$R\,\frac{T}{p_s}\,\nabla p_s$$

and this gives rise to significant aliasing associated with steep mountain slopes.

In practice, however, consequences of the above problem are difficult to detect. Initialisation introduces small changes which substantially reduce the erroneous divergence tendency and,when (as is usually the case in real applications) initialised fields have been interpolated to standard pressure levels, differences between results from the two choices of variable appear to be insignificant.

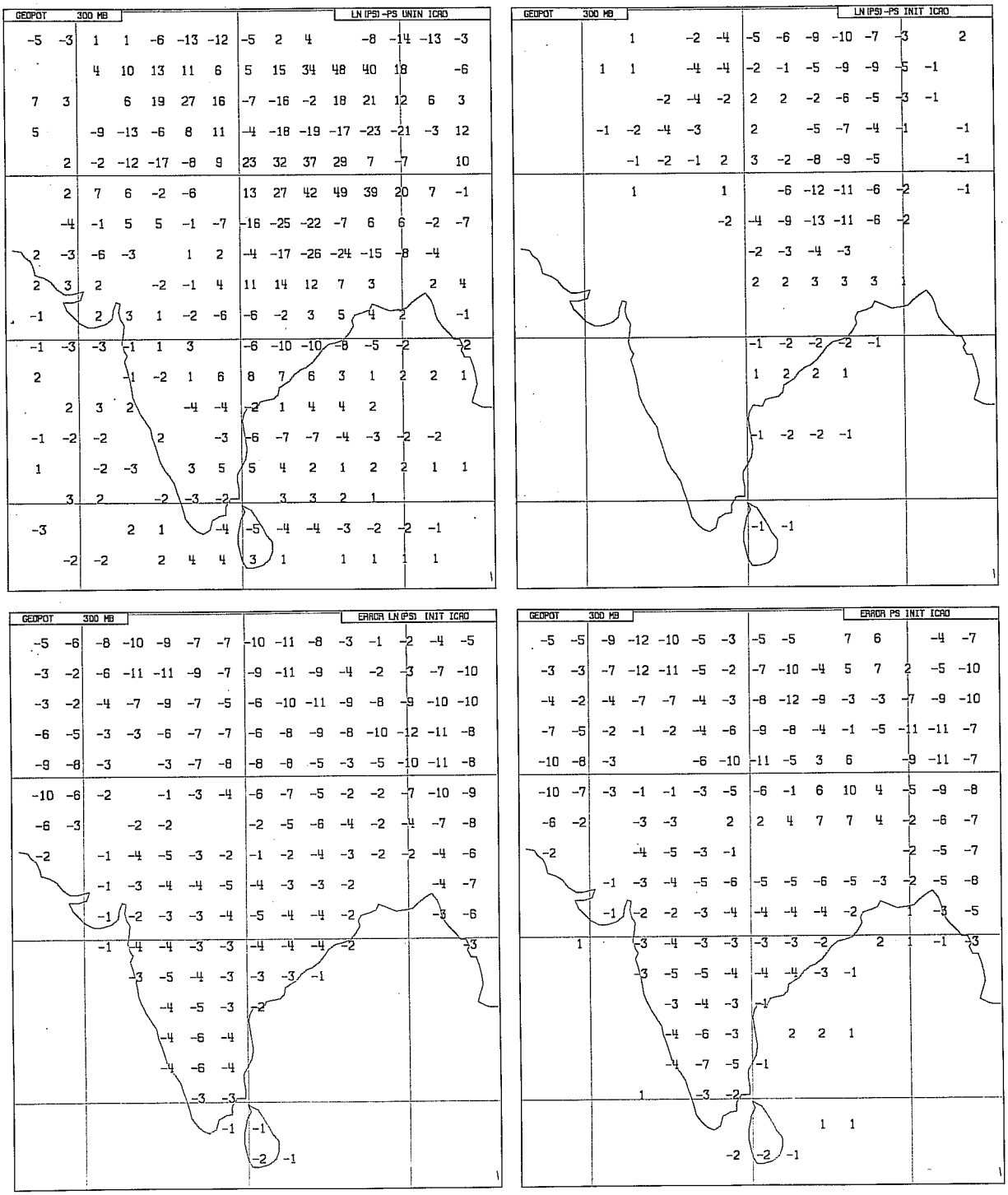

Fig. 7 Differences in 300 hPa height (m) plotted at model grid-points, derived from analytically-prescribed fields. Details are given in the text.

This point is illustrated in Figure 7 for the 300 hPa height field over and near the Indian subcontinent where aliasing problems tend to be largest (associated with the steep slopes of the southern flank of the Tibetan Plateau). Results are presented for T63 horizontal resolution, the second operational spectral orography with 16-level resolution and the hybrid vertical coordinate, and initial conditions are computed on the model Gaussian grid for the ICAO standard atmosphere. The upper left panel shows differences in the 300 hPa heights computed at model grid-point using $\ell n p_s$ and p_s as variables. These heights are evaluated following spectral fitting of the analytical temperatures and surface pressures, use of the model's difference scheme to compute geopotential at model half levels, and use of the standard operational post-processing to interpolate vertically to the 300 hPa level. Differences reach a maximum of 49 m. The upper right panel shows that differences are much reduced when the intermediate spectral fields are initialized by the nonlinear normal-mode technique. The analytical value of the 300 hPa height is known, and the lower two panels show the errors of the initialized heights for the $\ell n p_s$ and p_s schemes. There is little to choose between the two. In this idealized case initialisation increments are larger for the p_s scheme, but a data assimilation trial has revealed very little difference after 4 analysis cycles. Medium-range forecasts experiments also show a very low sensitivity to the choice of prognostic variable.

4. ENVELOPE OROGRAPHY AND GRAVITY-WAVE DRAG

Recent work on the parameterization of gravity-wave drag is discussed by Miller and Palmer in this volume. Objective verification of medium-range forecasts carried out using mean and envelope orographies, and with and without gravity-wave drag, has shown that best results are currently attained (at least at T106 resolution) by using a combination of envelope orography and the wave-drag parameterization; this combination has been adopted for operational forecasting. However, the verification also showed that the gravity-wave drag scheme had a larger beneficial impact when used with mean orography than when used with the envelope. It is of interest to examine this impact from a synoptic viewpoint.

The case chosen for purposes of illustration is one from the sequence of experiments discussed by Jarraud et al. in these proceedings. The initial date is 15 October 1983, and the subsequent evolution of the model atmosphere

reveals sensitivity to orography in both the position of a low over Siberia and the development of a depression in the lee of the Alps. Operational T63 analyses provided the initial conditions for the forecasts and are used for verification. T106 resolution, using either the currently operational one standard-deviation envelope orography or mean orography, was used for the forecasts.

Maps of 500 hPa height for the two-day forecasts are presented in Figure 8 for a region east of the Caspian Sea. The comparison of the mean- and envelope-orography forecasts carried out without gravity-wave drag reveals the more northerly (and more correct) position of the low in the forecast with envelope orography, as discussed by Jarraud et al. (cf their Figure 9). Including the parameterization of gravity-wave drag with mean orography can be seen to result in a northward shift of the low, although it remains to the south of the position with envelope orography. Adding gravity-wave drag to the forecast with envelope orography gives a much smaller improvement.

Day-3 forecasts of the Mediterranean cyclone are presented in Figure 9. Here there is little sensitivity to the inclusion of gravity-wave drag, although it gives rise to a slight fall in surface pressure over Southern Italy for both mean and envelope orography, thereby slightly increasing forecast accuracy in both cases. Sensitivity to the change from mean to envelope orography is more pronounced.

A larger impact of gravity-wave drag is seen in maps of 850 mb wind for day 5 shown in Figure 10. The change from mean to envelope orography results in a more westerly, and more accurate, position for the cyclonic centre over the Mediterranean. Including the parameterization of gravity-wave drag gives rise to a similar shift in position. This occurs for both orographies, with accuracy highest for the combination of envelope orography and gravity-wave drag. With mean orography the drag parameterization also results in a clear shift of the flow maximum over Southern France from the southwestern Alps to the vicinity of the Golfe du Lion, and this gives a flow distribution rather close to that found with envelope orography and no gravity-wave drag. A forecast with mean orography in which the parameterization was changed so as to give a larger low-level component to the drag shows an even more apparent "barrier" effect of the Alps.

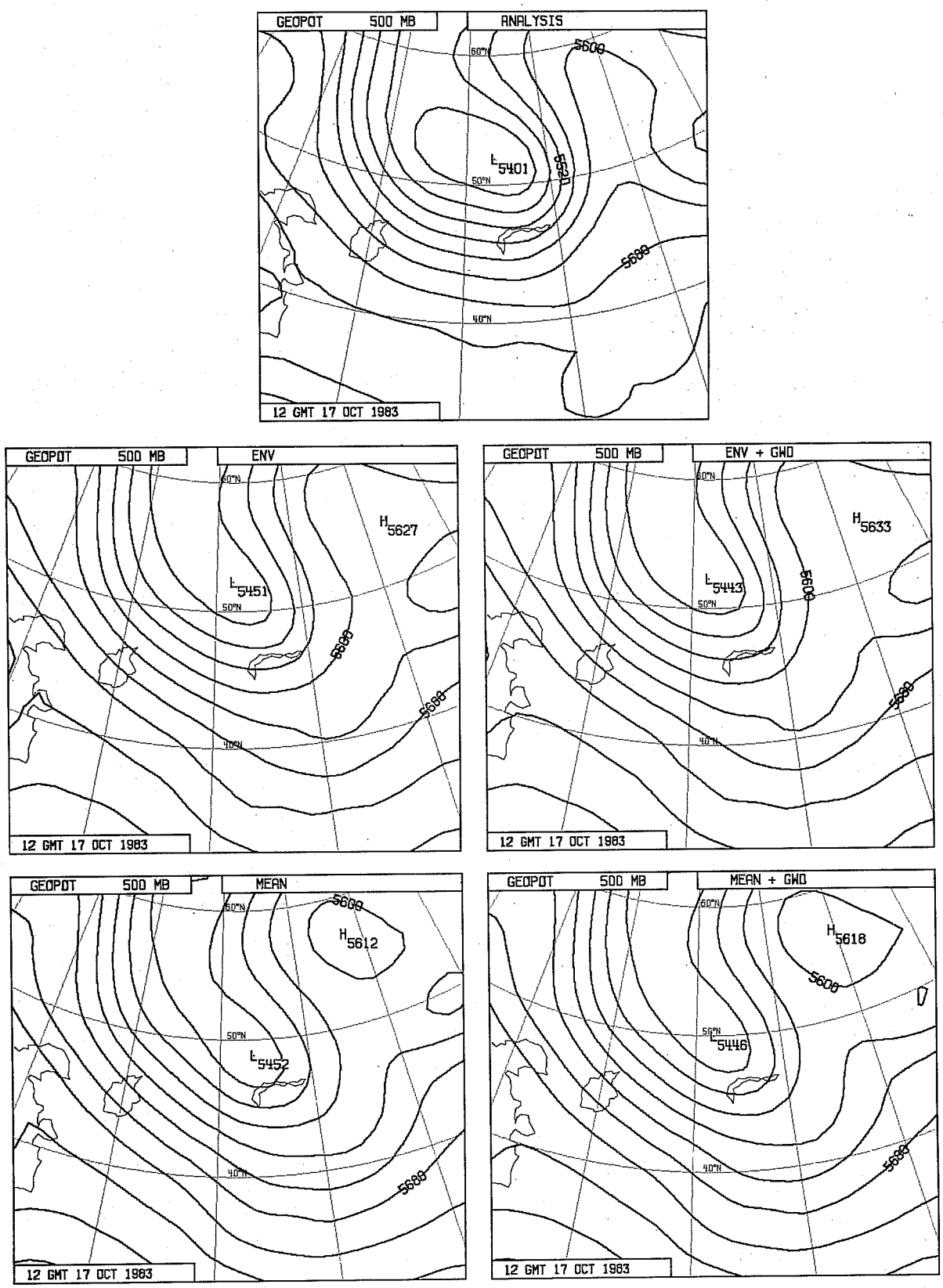

Fig. 8 The verifying analysis (upper) of 500 hPa height east of the Caspian Sea for 12Z, 17 October, 1983 and 2-day forecasts with
middle left : envelope orography without gravity wave drag
middle right: envelope orography with gravity wave drag
lower left : mean orography without gravity wave drag
lower right : mean orography with gravity wave drag

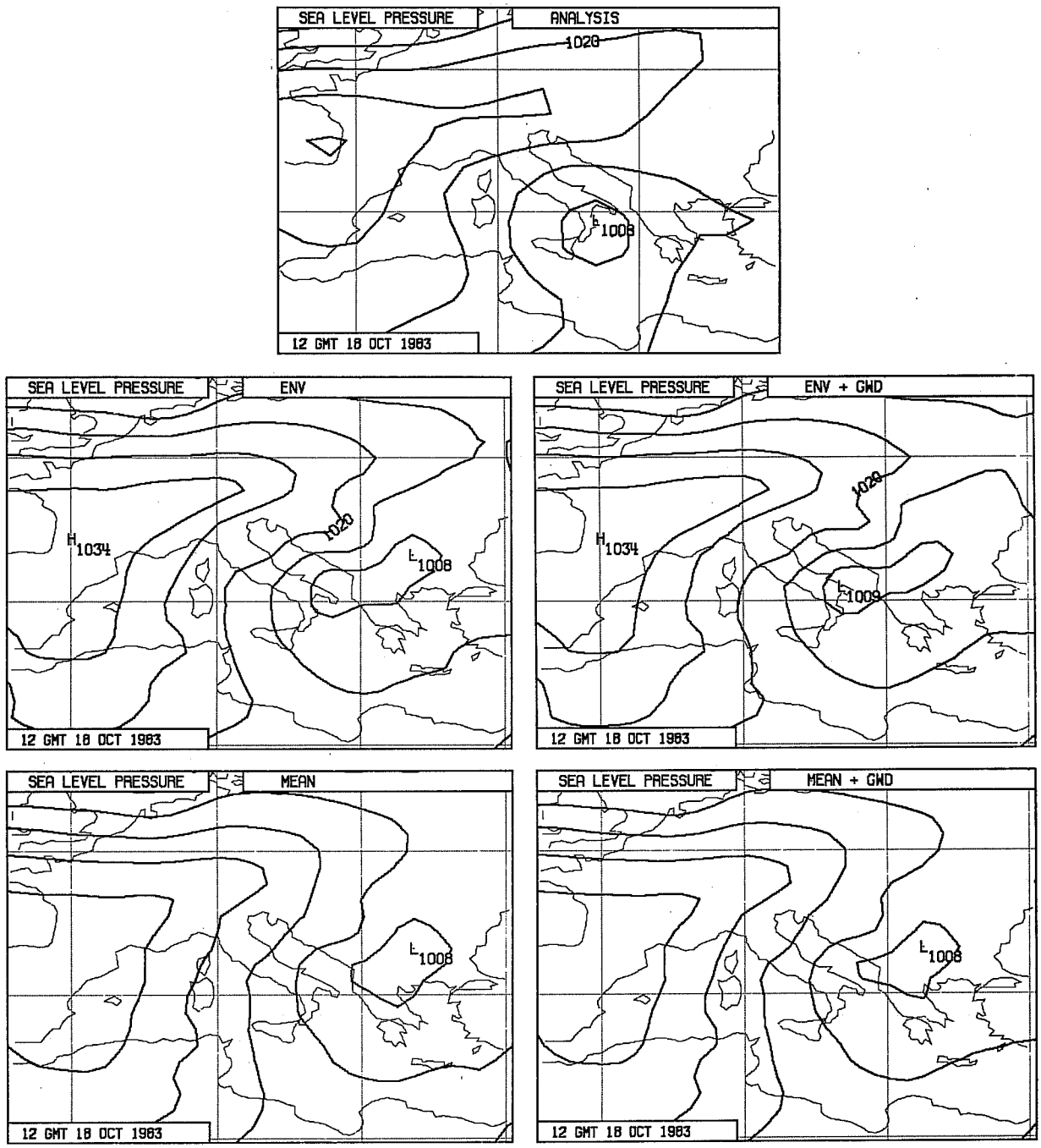

Fig. 9 The verifying analysis (upper) of mean sea-level pressure for 12Z, 18 October, 1983 and 3-day forecasts with
middle left : envelope orography without gravity wave drag
middle right: envelope orography with gravity wave drag
lower left : mean orography without gravity wave drag
lower right : mean orography with gravity wave drag

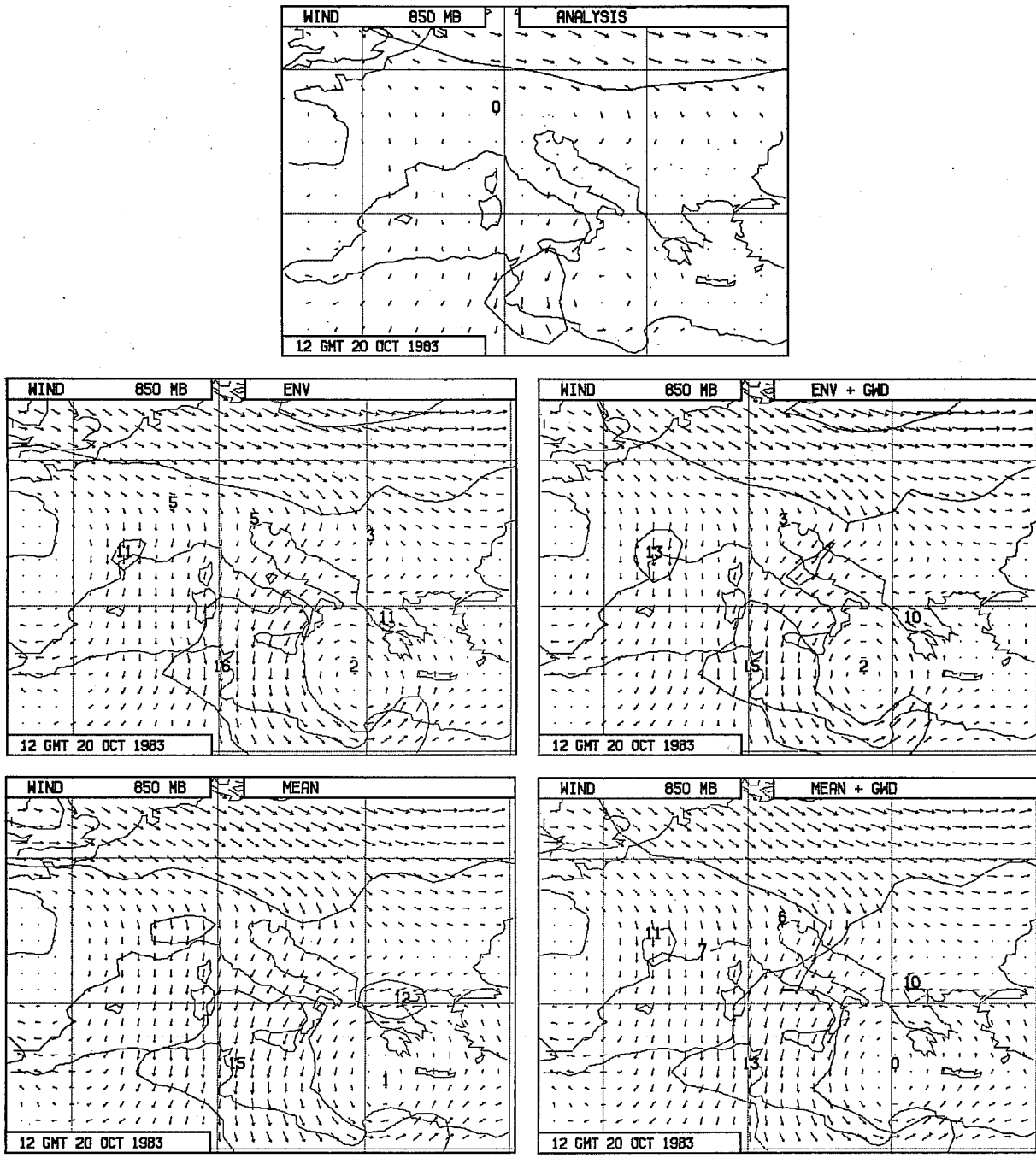

Fig. 10 The verifying analysis (upper) of 850 hPa wind for 12Z, 20 October, 1983 and 5-day forecasts with
middle left : envelope orography without gravity wave drag
middle right: envelope orography with gravity wave drag
lower left : mean orography without gravity wave drag
lower right : mean orography with gravity wave drag

Synoptic assessment of other cases has led to generally similar results. Miller and Palmer have discussed how objective verification for the Northern Hemisphere reveals a more accurate prediction of zonal wavenumbers one to three with envelope than with mean orography (in the absence of gravity-wave drag), and little impact of the gravity-wave drag on these scales when envelope orography is used. However, a pronounced impact, similar to that of a change to the envelope, is found when the gravity-wave drag is used with mean orography.

The above results suggest that mean orography plus a parameterization which gives a larger low-level drag than does the current scheme could well give better overall performance than the present combination of envelope orography and gravity-wave drag. The ability to vary the amount of drag according to the direction of the low-level flow and nature of the sub-gridscale orographic variability may be crucial in this respect. Investigation of this possibility is continuing.

It is appropriate here also to comment on the performance of different orographic representations in extended-range simulations. Figure 11 presents mean 1000 mb heights computed as an average of three 90-day T42 simulations starting from analyses for 6 December for the years 1983, 1984 and 1985. Results from several different model versions are presented, and for comparison a climatology computed from corresponding 90-day mean analyses for the winters 1980 to 1986 is also shown. The model versions are:

- a basic run with ($\sqrt{2}$ standard-deviation) envelope orography, no gravity wave drag and the formerly operational 16-level vertical resolution (upper right);
- a similar 16-level run but using a finite-element scheme (an extension of work reported by Burridge et al. (1986) and Steppeler (1986)) rather than finite differences for the vertical discretisation (middle left);
- a run using the current 19-level vertical resolution and finite-difference scheme (middle right);
- a similar run with the operational parameterization of gravity-wave drag included (lower left);
- a 19-level run with mean orography and no gravity wave drag (lower right).

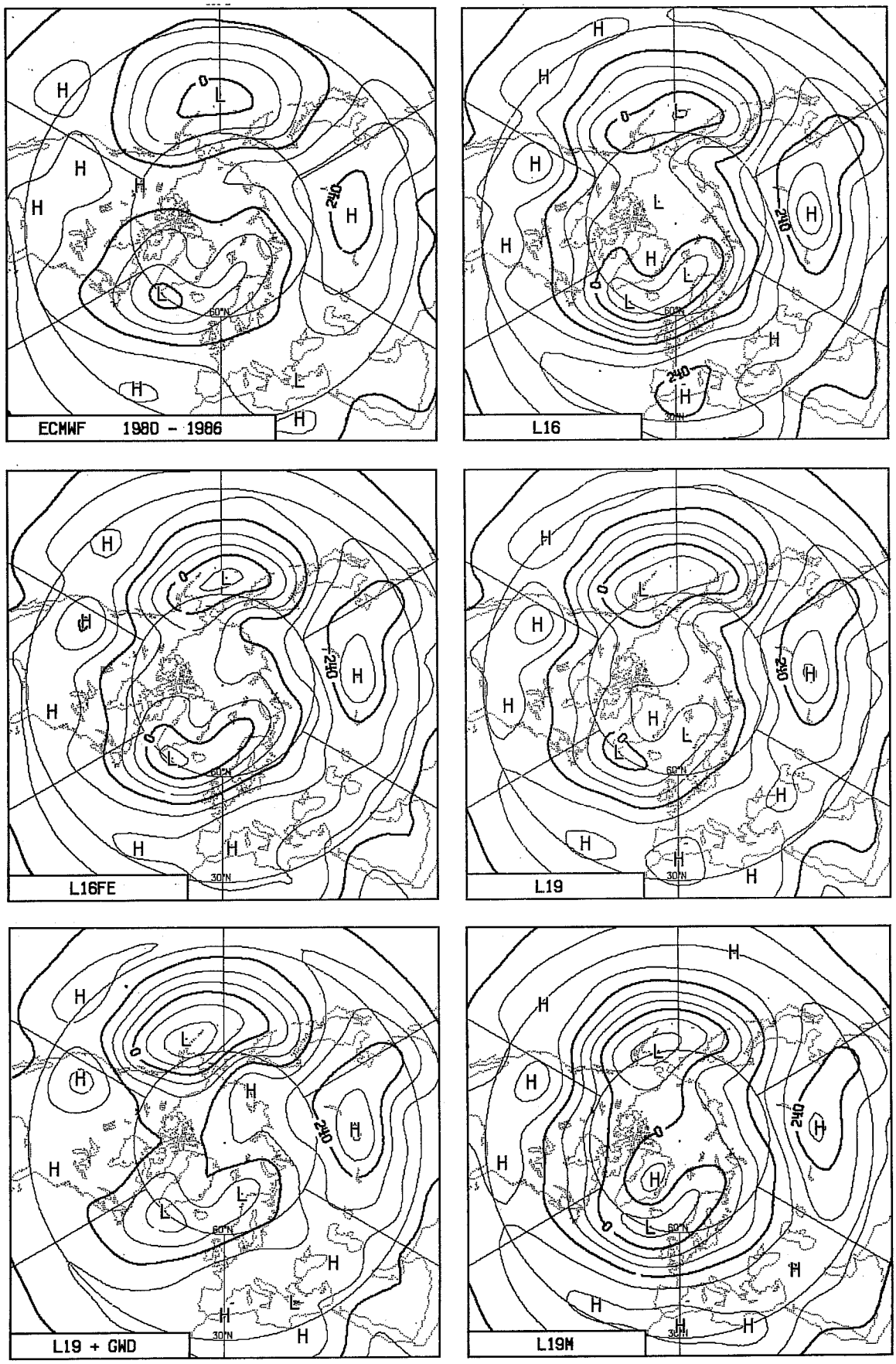

Fig. 11 A winter climatology of 1000 hPa height (upper left) and 5 model simulations specified in the text

Figure 11 illustrates how a change in numerical scheme, increased stratospheric resolution, use of envelope rather than mean orography, and introduction of a parameterization of gravity-wave drag, can bring about improvements in model climate which are, qualitatively at least, of a similar nature. In particular, each change acts to reduce the intensity of the predominantly westerly circulation over North-western Europe, Asia and North America. The sensitivity of model climate to such changes has been found in previous studies of the individual impact of one or other of them (e.g. Burridge et al. 1986; Boville (personal communication); Wallace et al. 1983:; Palmer et al. 1986), but Figure 11 serves as a reminder of the caution that should be exercised in, for example, fine-tuning an orographic representation to improve the climate of a model with inadequate stratospheric resolution.

5. HIGHER HORIZONTAL RESOLUTION

Increases in horizontal resolution have undoubtedly played a substantial rôle in the improvement of numerical weather prediction over the years. For the resolutions currently used for global forecasting, the representation of some synoptically-important mountain barriers remains deficient, and the analysis of observed data and direct application of model output in mountainous regions still pose problems. Attention thus continues to be directed towards exploring the benefits of increased horizontal resolution, with emphasis on the performance of models near orography. As an illustration of potential improvements in representation, Figure 12 shows Alpine cross-sections for mean and one standard-deviation envelope orographies at T106, T159 and T213 spectral resolutions. Increased computational power would also make possible increased vertical resolution, thus making it feasible to explore alternative approaches such as the "step mountains" discussed by Mesinger in these proceedings.

Experience with limited-area modelling already provides examples of local improvement due to increased horizontal resolution (e.g. Dell'Osso, 1984). Global experimentation at a resolution higher than T106 has recently begun at ECMWF, and some results from the first case studied are presented here. The initial date of 20 March 1986 was chosen because of an Alpine lee cyclogenesis early in the forecast range which was underestimated by the operational T106 forecast. A horizontal resolution of T159 was chosen since it was the largest that could run efficiently within the memory constraints of the Centre's computer system, albeit over too long a time to be operationally practical.

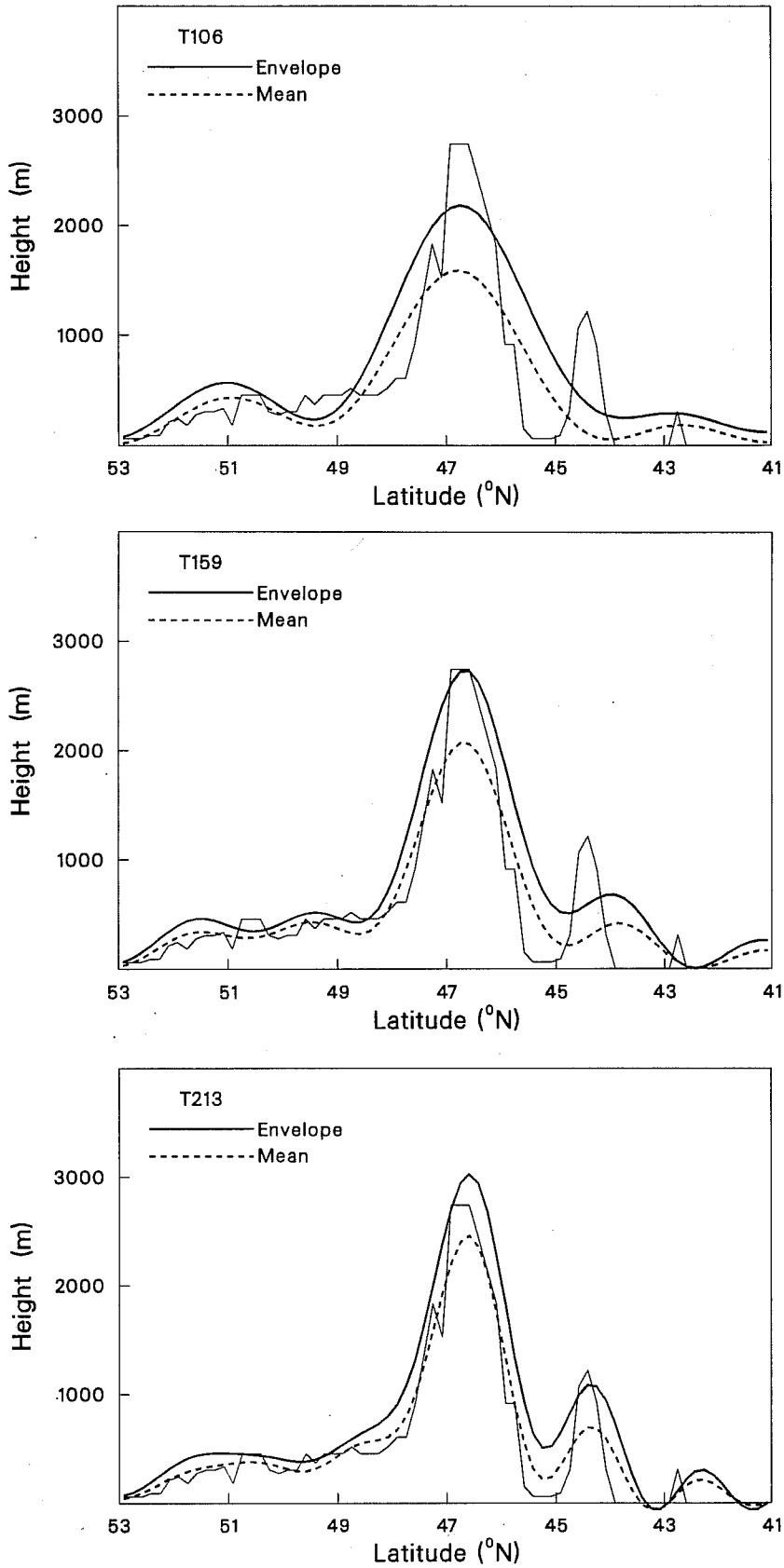

Fig. 12 Alpine cross-sections as in Fig. 1, but for mean and one standard-deviation envelope orographies and spectral truncations T106 (upper), T159 (middle) and T213 (lower).

A one standard deviation envelope orography was used, and initial data were interpolated from the operational T106 analysis.

One-day sea-level pressure forecasts, using T63, T106 and T159 resolutions, together with initial and verifying analyses are shown in Figure 13. A progressive improvement in the prediction of the lee cyclone as resolution increases is evident. Precipitation maps for the subsequent 24-hour interval, presented in Figure 14, not surprisingly show finer-scale structure at higher resolution. The T159 forecast improves over the other two in respect of heavy precipitation over Corsica and dryness to the north of the Adriatic, but appears to overestimate rainfall over the Italian peninsula and produces too much light rain over France.

Maps of 850 mb wind at day 5 are shown in Figure 15. All forecasts are broadly accurate over much of Europe, but the superiority of T159 is clear in its depiction of the lows over the Skaggerak and Norwegian Sea. Some differences of detail can be found elsewhere, but the general similarity of the low-level flow is more noteworthy. Despite this, quite distinct differences in the distribution of precipitation (almost certainly in part due to differences in orographic resolution) are found. Examination of the 24-hour precipitation totals shown in Figure 16 reveals a superiority of T159 in almost all respects.

As horizontal resolution increases, models can be expected to represent a larger degree of explicit orographically-induced gravity wave activity. Figure 17 presents cross-sections of wind and potential temperature at day 6 of T42, T63, T106 and T159 forecasts. Each section cuts through the Cascade and Rocky Mountain chains of western North America, although only T106, and to a greater extent T159, resolutions are capable of distinguishing between the two ranges. Over this area, the large-scale forecasts are rather insensitive to horizontal resolution when there is a predominantly westerly incident flow. Small-scale wave motion over and immediately downstream of the Rockies ridge is evident in the T159 forecast, but not at lower resolutions.

The forecasts discussed above were carried out without parameterization of gravity-wave drag. The Workshop discussions included in this volume raise the possibility that as resolution increases, effects of gravity waves which in

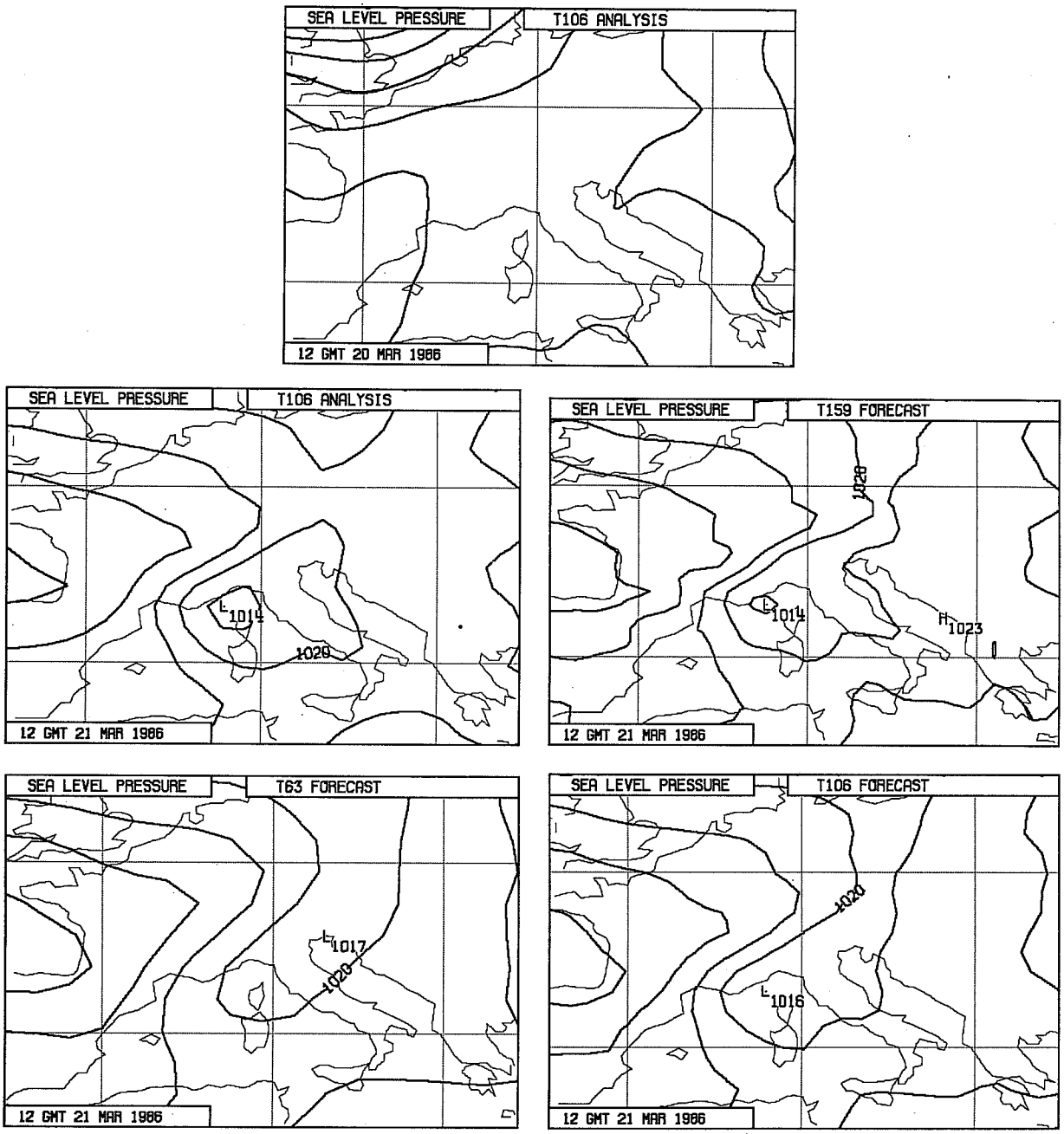

Fig. 13 Analyses of mean sea-level pressure for 12Z, 20 (upper) and 21 (middle left) March, 1986 and 1-day forecasts from 20 March using resolutions T159 (middle right), T63 (lower left) and T106 (lower right).

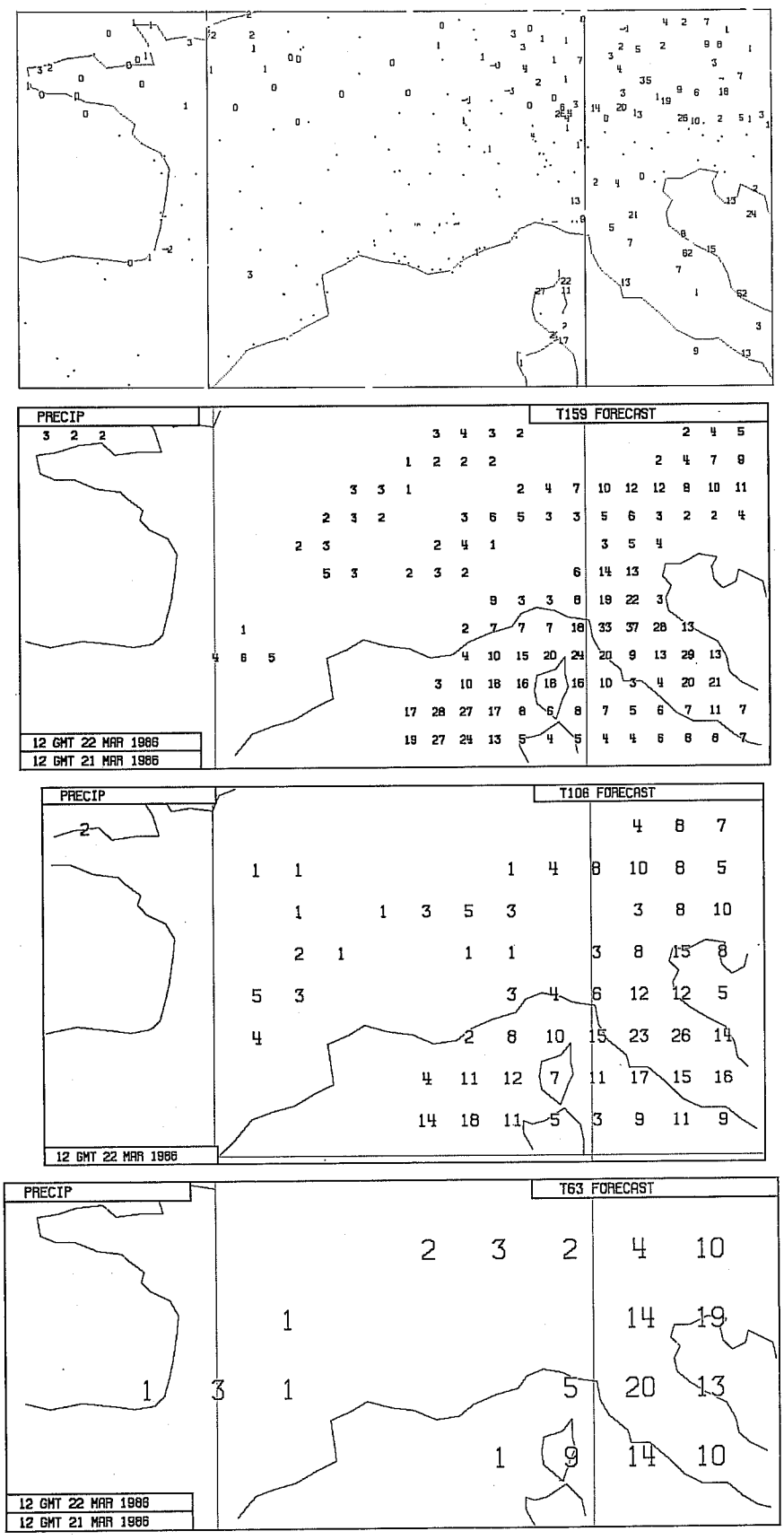

Fig. 14 24-hour net precipitation (mm) for the period 12Z, 21 March to 12Z, 22 March, 1986. Observed values are shown in the upper plot, a dot indicating no precipitation. Values for each model grid-square are shown for forecasts from 12Z, 20 March at resolutions T159 (upper middle), T106 (lower middle) and T63.

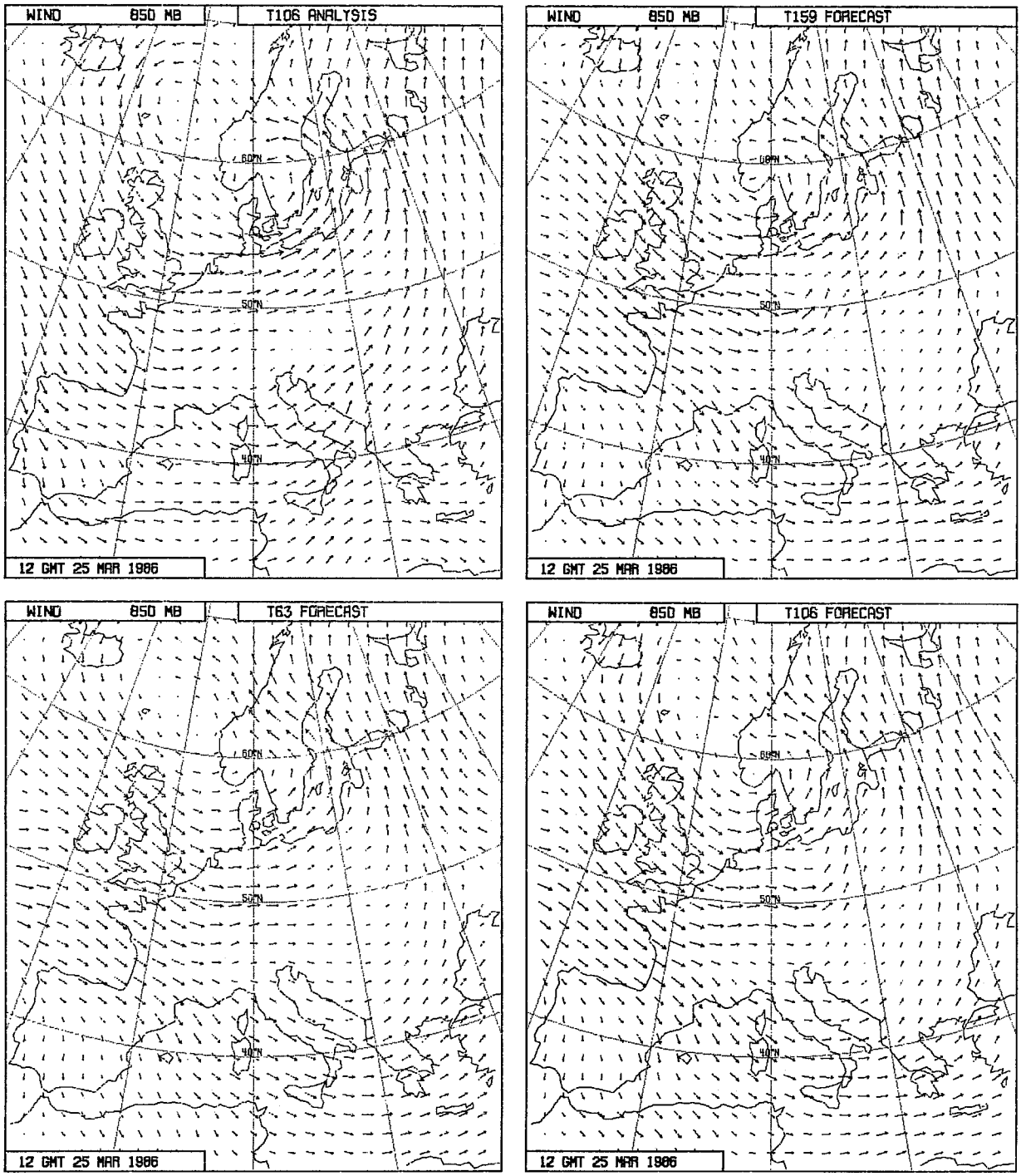

Fig. 15 Verifying analysis (upper left) of 850 hPa wind for 25 March 1986 and 5-day forecasts using resolutions T159 (upper right), T63 (lower left) and T106 (lower right).

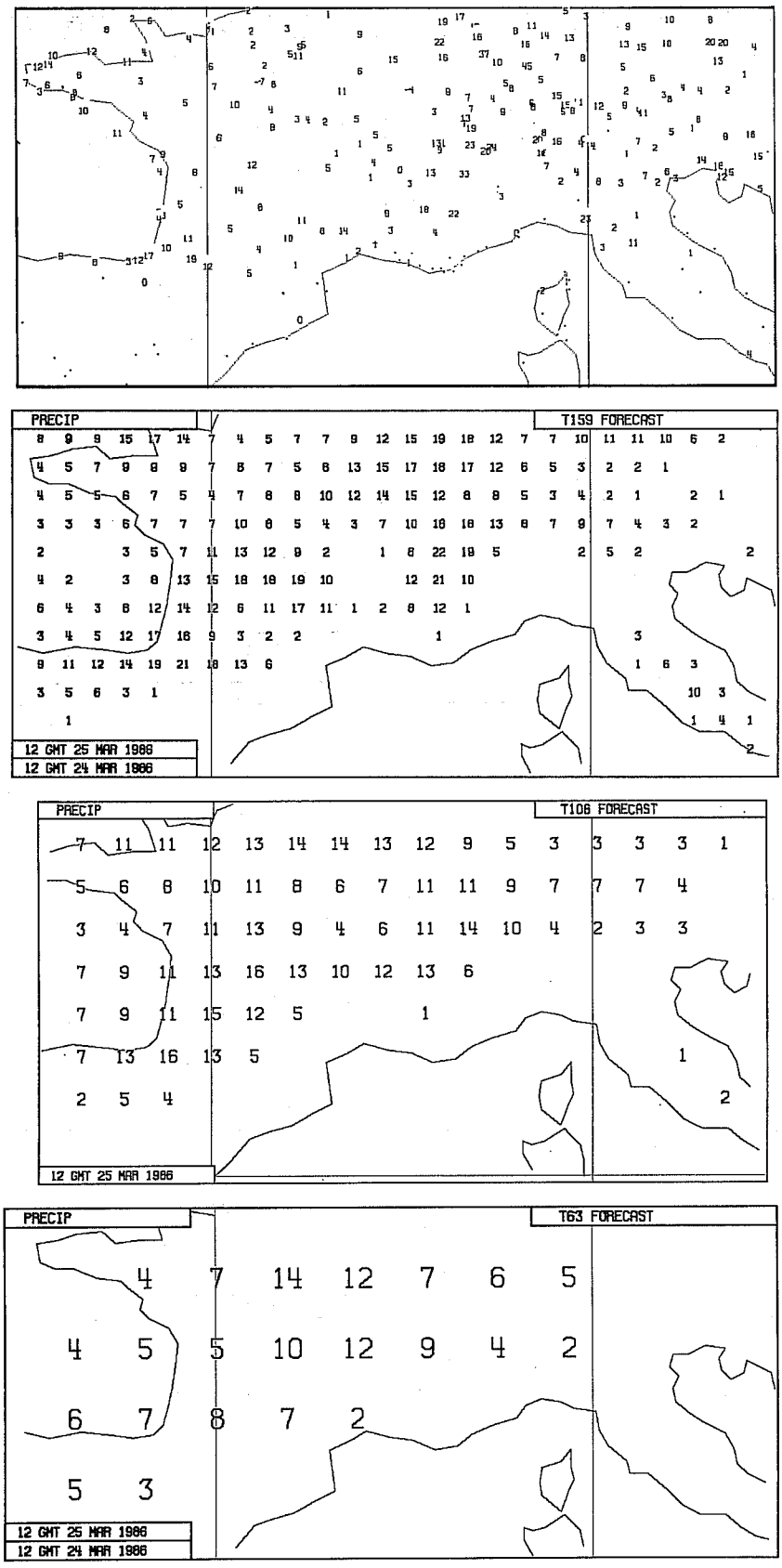

Fig. 16 24-hour net precipitation (mm) for the period 12Z, 24 March to 12Z, 25 March 1986. Observed values are shown in the upper plot, and forecast values are for T159 (upper middle), T106 (lower middle) and T63.

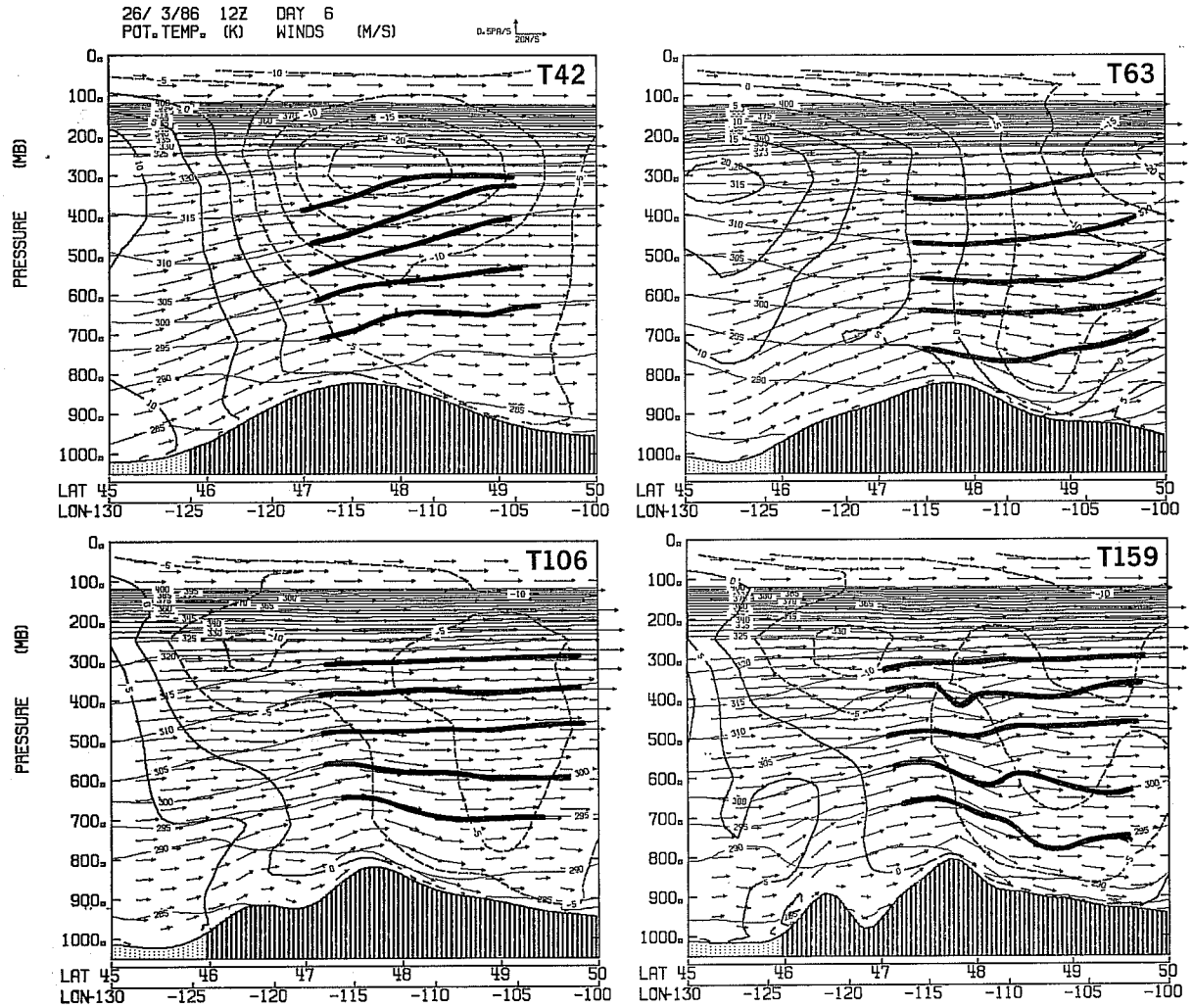

Fig. 17 Cross-sections of potential temperature and winds from 45°N 130°W to 50°N, 100°W for day 6 using resolutions T42 (upper left), T63 (upper right), T106 (lower left) and T159 (lower right).

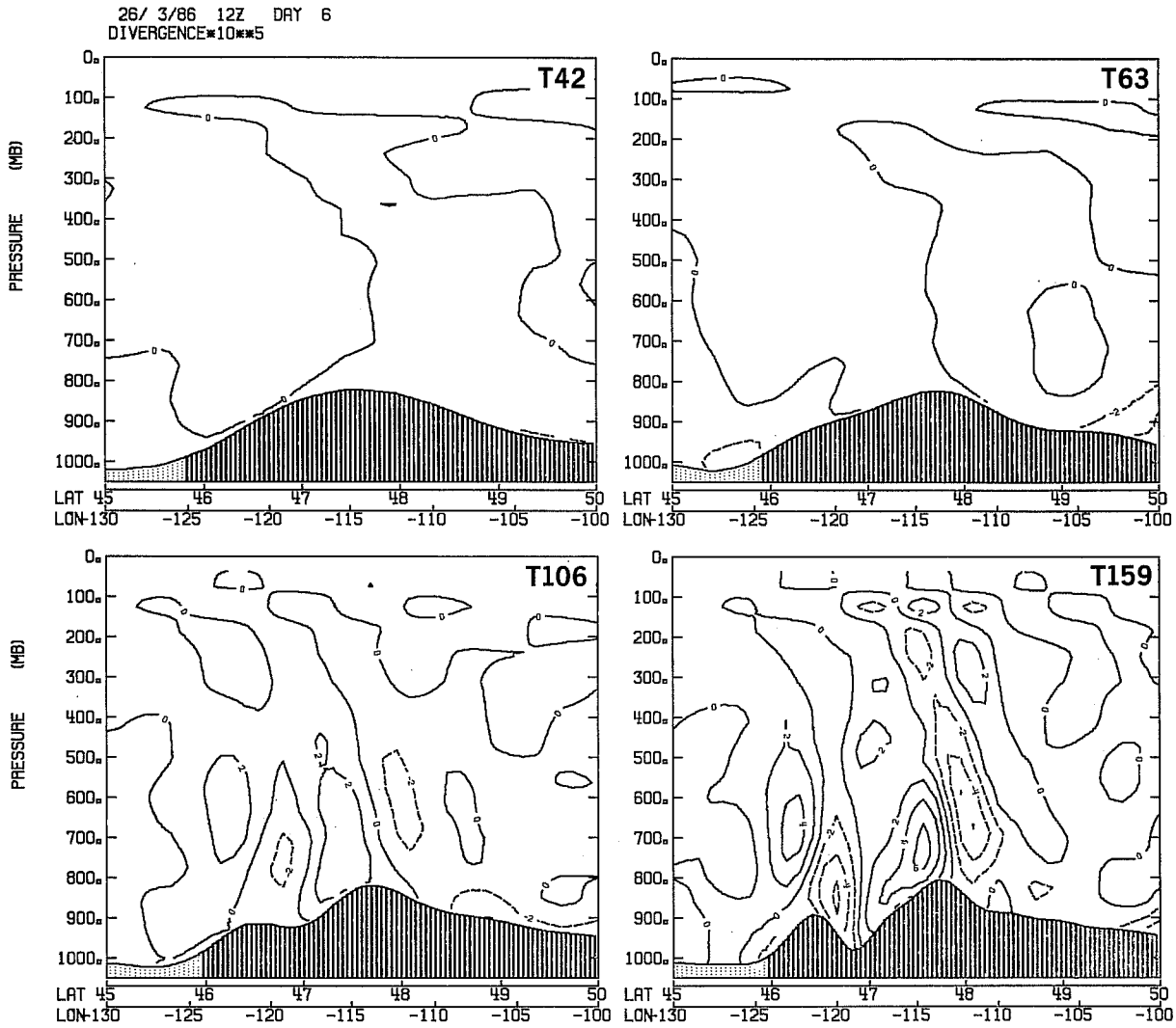

Fig. 18 Cross-sections of divergence from 45°N 130°W to 50°N 100°W for day 6 using resolutions T42 (upper left), T63 (upper right), T106 (lower left) and T159 (lower right).

reality occur on scales close to the truncation limit may appear twice in the model, once through parameterization and once explicitly. A related point, probably a minor one in view of the somewhat arbitrary nature of some aspects of the parameterization, is that the current practice at ECMWF of computing orographic variances about mean heights computed for the Gaussian grid, which has a finer resolution than the spectrally-fitted explicit model orography, results in the existence of a spectral range over which unresolved orographic variance is not taken into account in computing the generation of parameterised gravity waves.

Quite apart from the above problem, the explicit appearance of vertically-propagating gravity waves brings the question of the upper boundary condition to the fore. Cross-sections as in Figure 17, but for the divergence field, are presented in Figure 18. In the troposphere a westward phase tilt with increasing height can be seen over the Rockies at T159 resolution and for T106. However, the stratospheric detail evident for T159 shows an absence of tilt which is suggestive of an erroneous wave reflection due to the inadequate treatment of upward propagating waves in the topmost layers of the model. These forecasts were all carried out using the formerly-operational 16-level resolution. During testing of the increased stratospheric resolution of the present 19-level version, more extreme cases where strong mountain waves appeared explicitly at T106 and T63 truncations were examined. These showed a more severe problem of this nature at higher vertical resolution, with the occurrence at small horizontal scales of pronounced two-grid waves in the vertical at upper model levels. This led to the use of higher horizontal diffusion in the stratosphere of the operational 19-level model, an apparently effective remedy, at least for the short term, but one which should not be seen as obviating the need for a much more thorough study of this topic as horizontal and vertical resolution increase further.

6. CONCLUDING REMARKS

In this paper an account has been given of a variety of studies connected directly or indirectly with orography that have been carried as part of the development of ECMWF's global operational forecast model. Some of the topics covered have been the subject of many investigations reported in the scientific literature by different workers, while others have doubtless given cause for study at various weather prediction centres but have not appeared

prominently in formal publications. An attempt at a comprehensive review of experience elsewhere has not been made, but much of what has been discussed here is probably of quite widespread relevance.

In examining certain aspects of the numerical formulation, we have seen how progress has been made in a number of areas, although much of what has been presented must be seen as reducing or alleviating problems rather than as fundamental solutions. Concerning the representation of orographic effects, increasing resolution undoubtedly significantly eases some problems, but also leads to others becoming of greater prominence. Some of the discussion given here has been specific to spectral models, and as resolution increases the advantage of the global spectral technique over a technique based on a local representation may cease. A major new comparison of techniques with a view to possible operational change is an important element of the Centre's longer-term plans. Thus while orography is likely to remain one of the key areas of research in numerical weather prediction, and at the Centre in particular, emphasis in the future could well be differently placed.

Acknowledgement
Thanks are expressed to the many Staff Members and Visiting Scientists of ECMWF who contributed in some large or small way to the work reported here.

References

Berkofsky, L. and E.A. Bertoni, 1985: "Mean topographic charts for the entire Earth" Bull.Amer.Met.Soc., 36, 350-354.

Burridge, D.M. and J. Haseler, 1977: "A model for medium range weather forecasting - Adiabatic Formulation". ECMWF Technical Report No. 4, 46 pp.

Burridge, D.M., J. Steppeler and R. Strüfing, 1986: "Finite element schemes for the vertical discretization of the ECMWF forecast model using linear elements". ECMWF Technical Report No. 54, 51 pp.

Dell'Osso, L., 1984: "High resolution experiments with the ECMWF model: A case study". Mon.Wea.Rev., 112, 1853-1883.

Gordon, H.B., 1981 "A flux formulation of the spectral atmospheric equations suitable for use in long-term climate modelling". Mon.Wea.Rev., 109, 56-64.

Laprise, R., 1985: "Mass correction in a spectral GCM" in Research Activities in Atmospheric and Oceanic Modelling, Report No. 8, WMO, Geneva, 3.12-3.13.

Palmer, T.N., G.J. Shutts and R. Swinbank, 1986: "Alleviation of a systematic westerly bias in general circulation and numerical weather prediction models through an orographic gravity wave drag parametrization". Quart.J.Roy.Met.Soc., 112, 1001-1039.

Phillips, N.A., 1957: "A coordinate having some special advantages for numerical forecasting". J.Met., 14, 184-185.

Simmons, A.J., 1983: "Adiabatic formulations of the ECMWF forecasting system" in Proceedings of 1982 ECMWF Seminar/Workshop on the Interpretation of Numerical Weather Prediction Products, 59-81.

Simmons, A.J., and D.M. Burridge, 1981: "An energy and angular-momentum conserving vertical finite-difference scheme and hybrid vertical coordinates". Mon.Wea.Rev., 109, 758-766.

Simmons, A.J., and M. Jarraud, 1984: "The design and performance of the new ECMWF operational model" in Proceedings of 1983 ECMWF Seminar on Numerical Methods for Weather Prediction, Vol. II, 113-164.

Simmons, A.J., and R. Strüfing, 1981: "An energy and angular-momentum conserving finite-difference scheme, hybrid coordinates and medium-range weather forecasting". ECMWF Technical Report No. 28, 68 pp.

Steppeler, J., 1986: "Finite element schemes for the vertical discretization of the ECMWF forecast model using quadratic and cubic elements". ECMWF Technical Report No. 55, 59 pp.

Tibaldi, S., and J.-F. Geleyn, 1981: "The production of a new orography, land-sea mask and associated climatological surface fields for operational purposes". ECMWF Technical Memorandum No. 40.

Wallace, J.M., S. Tibaldi, and A.J. Simmons, 1983: "Reduction of systematic forecast errors in the ECMWF model through the introduction of an envelope orography". Quart.J.Roy.Met.Soc., 109, 683-717.

Wergen, W. and A.J. Simmons, 1986: "Experiments with increased vertical resolution in the ECMWF model" in Research Activities in Atmospheric and Oceanic Modelling, Report No. 9, WMO, Geneva, 4.1-4.4.